JPL Document D-35484

Terrestrial Planet Finder Coronagraph

TPF-C Technology
Milestone #1 Report

July 10, 2006

Editors:

John Trauger, Brian Kern, and Andreas Kuhnert

National Aeronautics and Space Administration

Jet Propulsion Laboratory
California Institute of Technology
Pasadena, California

Approvals

Released by

John Trauger   7/9/06

John Trauger
TPF-C High Contrast Imaging Testbed PI, JPL

Approved by

                               7/10/06
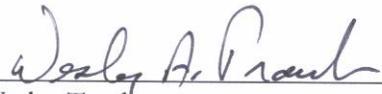
Marie Levine
TPF-C Systems Manager, JPL

                               13 July 2006.

Wesley Traub
TPF Project Scientist, JPL

                               7/12/06

Daniel Coulter
TPF Project Manger, JPL

                               7/11/06

Michael Devirian
Navigator Program Manager, JPL

                               14 July 2006

Zlatan Tsvetanov
TPF Program Scientist, NASA HQ

                               7/26/06

Lia LaPiana
TPF Program Executive, NASA HQ

TABLE OF CONTENTS

TERRESTRIAL PLANET FINDER CORONAGRAPH

TPF-C Technology Milestone #1 Report:
Narrow Band Starlight Suppression Demonstration

1.0   ABSTRACT

This document reports the achievement of TPF-C Technology Milestone #1, a demonstration of coronagraphic imaging contrast of 10^{-9} or better at distances from a central "star" of relevance for future planet finding missions, and a verification that our active wavefront sensing and control algorithms can maintain this contrast in hour-long data sets.

We note that our contrast metrics have met the milestone requirements, and nearly all meet these requirements with confidence limits greater than 0.99. Further, we note that the overall mean contrast values for the super-set of data are 6.9×10^{-10} and 5.7×10^{-10} in the specified inner (4–5 λ/D) and outer (4–10 λ/D) target dark fields respectively, again well within the contrast requirements.

We review the milestone specification from the Milestone White Paper (22 November 2005, attached to this document as Appendix 3), summarize the experiments performed in the High Contrast Imaging Testbed (HCIT), detail the procedures and a statistical analysis of the resulting data, and present representative data.

This document has been prepared by the TPF-C project for review by NASA HQ and the Navigator EIRB.

2.0   INTRODUCTION

The primary objective of the Terrestrial Planet Finder Coronagraph mission is the direct imaging of earth-sized planets orbiting the nearby stars, requiring a significant advancement in technology beyond current space imaging capabilities. It is envisioned that the critical elements of technology will be identified and that a sequence of performance milestones will be defined that lead ultimately to an overall validation of the TPF-C concept. This first TPF-C Milestone addresses coronagraphic starlight suppression in narrowband light. As specified in the M1 White Paper, the milestone reads as follows: *"Demonstrate that the High Contrast Imaging Testbed (HCIT) achieves a baseline contrast of 1×10^{-9} (goal 1×10^{-10}) at a $4\lambda/D$ inner working angle, at a wavelength of 785 nm and stable for at least one hour."* We anticipate that future milestones will extend this first demonstration in the directions of deeper contrast, spectral bandwidth, and fidelity of engineering models.

This metric addresses several key aspects of the TPF-C performance error budget. TPF-C is required to form a high contrast "dark field" over a working angle spanning 4–40 λ/D and a bandwidth of 500–800 nm. An extensive TPF-C modeling effort has shown that it is increasingly difficult to drive down the contrast of the dark field as one moves toward the image of the target star. The HCIT addresses the most challenging location in the image plane, the inner working angle, at the same location required by TPF-C. The outer working angle for the flight mission is achieved

using a large (at least 96 × 96 actuator) deformable mirror (DM). HCIT currently operates with a 32 × 32-actuator DM, so it controls a smaller region (to a radial distance 10 λ/D). This field is sufficiently large that the physics of the wave front control problem can be demonstrated with high expectation of applying the same approach to a larger dark field at a later date.

TPF-C must be sensitive to light reflecting from planets with intensity 10^{-10} fainter than that of the parent star. Ideally this is achieved by driving all scattered light surrounding the star to an intensity contrast ratio below 10^{-10}. M1 requires an HCIT contrast demonstration to the 10^{-9} level. By achieving this result, HCIT will have demonstrated performance that is limited not by the instrument but by the nature of the target.

Narrowband speckles in the dark field resemble classic laser speckles with intensities that follow a negative-exponential distribution. The statistical distribution of intensities has a long tail; that is, there are bound to be a few very bright speckles. This is accounted for in the TPF-C performance error budget and is a measured and expected result in HCIT. Because of this, the contrast specification relates to the average contrast level in the areas of interest around the source or parent star.

3.0   HCIT OVERVIEW

The milestone demonstration has been carried out with the High Contrast Imaging Testbed (HCIT), a laboratory facility presently located in the JPL Optical Interferometry Demonstration Laboratory. The testbed supports the development of two fundamental elements of the baseline high-contrast imaging strategy for TPF-C. These are (1) suppression of scattered light via wavefront control with a single DM and speckle nulling at the science camera, and (2) suppression of diffracted light via a Lyot coronagraph with a band-limited focal plane occulter. Other configurations are planned for future demonstrations, including wavefront control with multiple DMs in the optical path and diffraction control using alternate coronagraph configurations.

The HCIT is an outgrowth of eight years of development at JPL of the actively-controlled space coronagraph concept for the exploration of the nearest exo-solar planetary systems. Conceived at the beginning as a "skunkworks" for the early development of coronagraph technologies, algorithms, and predictive models, the HCIT uses as much as possible inexpensive off-the-shelf optical and electronic components. Initial experiments in 1998 involved prototypes of the modular DMs, based on PMN electrostrictive technology at Xinetics and supporting control electronics and algorithms, mounted on a Michelson interferometer "surface gauge", mounted in a vacuum and capable of directly imaging the DM surface with 0.1 × 0.1 mm resolution (100 pixels per actuator) and 10 pm accuracy for surface deviations. This DM development, supported over the past eight years by a number of SBIR grants to Xinetics and technology funding at JPL, leveraged the PMN electrostrictive technology widely in use in discrete-actuator deformable mirrors at ground based observatories. Surface figure control demonstrations at the 25 picometer rms level, together with optical Fresnel propagation models for a variety of Lyot coronagraphs and speckle nulling algorithms, indicated that the wavefront control technology was ready for demonstrations of high-contrast imaging in a dedicated coronagraph testbed (Trauger et al. 2002). Coronagraph elements were first assembled on the optical table in 2002 and initial experiments were carried out without a vacuum chamber in the ambient laboratory. The optical table (as well as the original Michelson "surface gauge") was moved to its present location and installed in the vacuum chamber in 2003.

The HCIT now facilitates high contrast demonstrations in support of TPF-C and supports outside experimenters from the larger TPF community outside of JPL. Upgrades of the testbed optics are anticipated for future high-contrast imaging demonstrations approaching the level of TPF-C flight requirements.

3.1   HCIT Optical Layout

The coronagraph optics are mounted on a 5 × 7 foot optical table, which is supported on elastomeric vibration isolation blocks within a cylindrical vacuum chamber measuring 6 feet in diameter and 8 feet in length. The vacuum chamber is supported and vibration isolated from the laboratory floor by six pneumatic isolation legs, and during operation is evacuated to approximately 1 milliTorr with a dry scroll pump. The chamber walls are wrapped with a thermostatically controlled heating tape and a thermal blanket to maintain the chamber walls at temperature a few degrees above ambient, and constant to within 0.3 degrees C. The optical layout is illustrated in Figure 1.
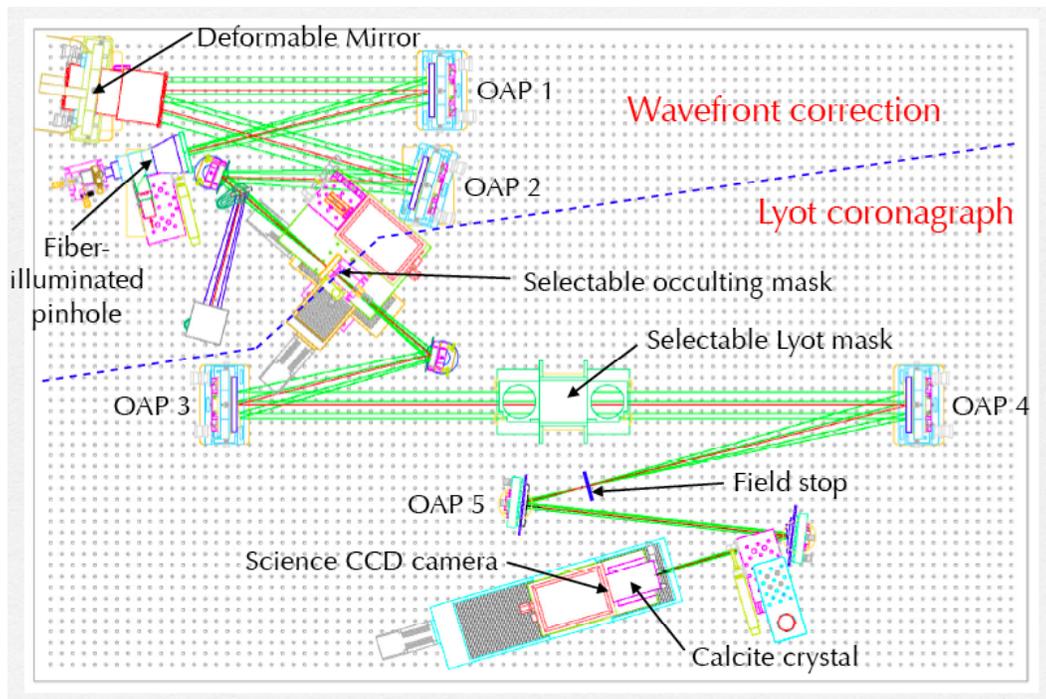

Figure 1. The HCIT coronagraph layout. *The essential elements of the optical system are the light source (simulated star image), off-axis parabolic (OAP) relay mirrors, a 32× 32 mm deformable mirror, coronagraph occulter and Lyot stop mounted on motorized stages for selection and alignment, a field stop, a calcite prism for discrimination of polarization, and the science CCD camera. All mirrors have unprotected gold coatings.*

With reference to Figure 1, the elements located at upper left prior to the occulting mask perform the wavefront correction, relaying the pinhole light source to the occulting mask and ultimately correcting a $\lambda/10$ rms wavefront to the levels required for high contrast.

The light source for these experiments is a Newport LD-785-61C fiber-coupled laser diode, driven by a Model 500 diode driver and Model 350 temperature controller. The diode controller is pulsed under computer control to provide exposure times as short as 30 microseconds. As indicated

in Figure 2, the light output from the diode is transmitted by a single-mode fiber through the wall of the vacuum chamber to the optical table, where a pair of lenses re-images light from the tip of the fiber to a 5-micron diameter pinhole. This pinhole provides both the simulated "star" and a dark surrounding field. The illumination pattern from the pinhole, as measured at the first off-axis parabolic mirror (OAP1), is non-uniform at the 10-15% level due to the combined effects of the fiber radiation pattern, pinhole diffraction, and small misalignments. Polarization of the pinhole illumination is not actively controlled. Experience has shown that the plane of polarization, as measured in the final CCD focal plane, drifts by no more than a few degrees of rotation per day.
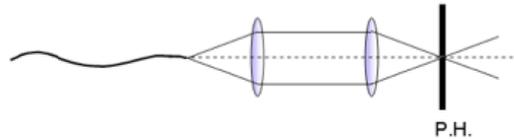

Figure 2. Fiber-illuminated pinhole light source.

The source pinhole is reimaged on the coronagraph occulter with the following optical elements. OAP1 and OAP2 are commercial off-the-shelf mirrors from SORL with identical specifications (OAP 30-05.75-03.5SQ, 30 inch focal length, 3.5 inch diameter, $\lambda/16$ rms surface accuracy). The fold flat has $\lambda/100$ rms surface quality. The deformable mirror is manufactured by Xinetics Inc. It is a monolithic array of 1024 PMN electroceramic actuators, in a 32×32 square array, with an actuator pitch of 1 mm. The mirror facesheet is polished to $\lambda/100$ rms. A 30 mm diameter black-anodized aperture is placed in close proximity to the DM, defining the system pupil. The actuator driver system includes a control computer, a power supply, multiplexer driver, digital-to-analog converters (DACs) and clocking circuits which feed a set of low-power low-leakage multiplexer switch arrays in close proximity to the DM inside the vacuum chamber. A 30 mm diameter pupil stop mounted near the DM surface is the defining pupil aperture for the experiment. Control computers and driver electronics reside outside the vacuum chamber. The reflective surface on all mirrors is unprotected gold, with reflectances uniform over the surface at the level of a few percent. These non-uniformities in wavefront amplitude due to mirror reflectances and the pinhole illumination pattern are significant contributors to the overall wavefront imperfections that must be corrected with our wavefront control algorithm.

The elements from the coronagraph occulter to the science camera perform the suppression of diffracted light with a Lyot coronagraph, described in more detail in the Section 3.2. The beam is collimated by OAP3, which also projects an image of the DM and its pupil stop to the plane of the Lyot stop. OAP4 brings the light to a focus at the location of the field stop. These OAP3 and OPA4 are identical to OAP1 and OAP2. The final two off-axis parabolic mirrors OAP5 and OAP6 relay the image to the focal plane with a 3:1 magnification. The science focal plane is an e2V 1033×1056 pixel, back-illuminated and AR-coated CCD, cooled thermoelectrically to $-70°$ C. A beam-displacing calcite prism (Lambrecht MBDS20, AR coated, measuring $45 \times 20 \times 20$ mm) deviates one of the polarization components to create a pair of images separated by 4.7 mm on the CCD. Only one of these images (the deviated, extraordinary ray) is used throughout this milestone demonstration. This selection is arbitrary and inconsequential for the milestone demonstration. Though not a part of this report, we note that experimentation with HEBS (next section) occulters has shown no measurable dependence on polarization, such that speckle nulling in either of the two polarizations creates identical high-contrast dark fields in both polarizations. All imaging in the HCIT is performed at this

single focal plane, including all wavefront sensing and correction and the recording of high contrast images.

3.2   Elements of the Lyot Coronagraph

The HCIT coronagraph configuration for this milestone demonstration is a Lyot coronagraph with band-limited occulter. The concept of a band-limited coronagraph was introduced by Kuchner and Traub (2002). The specific HCIT occulter element used for this demonstration has a fourth-order sinc^2 profile. The occulter was written at JPL's Micro Devices Laboratory, where a 100-keV electron lithography system was used to create a continuous grey-scale attenuation profile in lithography-quality HEBS (high energy beam sensitive) glass supplied by Canyon Materials Inc. (Wilson et. al 2002). The specific analytic form of the occulter transmittance is shown in Figure 3a, and the measured transmittance is illustrated in Figure 3b and 3c. This attenuation profile gives rise to a weak pattern of phase shifts, which is ultimately corrected by our wavefront control algorithm. The occulter substrate is 0.090 inch thick, with no AR coatings, tilted 5 degrees about the horizontal axis so that light reflected from the occulter can be collected by a beam-dump. The corresponding Lyot stop, shown in Figure 3d, is formed from a pair of black-anodized aluminum plates, each with a circular aperture of the same diameter as the defining pupil stop mounted with the DM.

$$T(x) = \left[1 - \left(\frac{\sin(\pi \varepsilon x D / 2\lambda f)}{\pi \varepsilon x D / 2\lambda f}\right)^2\right]^2$$

(a)

(b)

(d)

$\leftarrow (1-\varepsilon) D \rightarrow$

(c)

$\leftarrow 8 \lambda/D$ FWHM

Meas
Spec
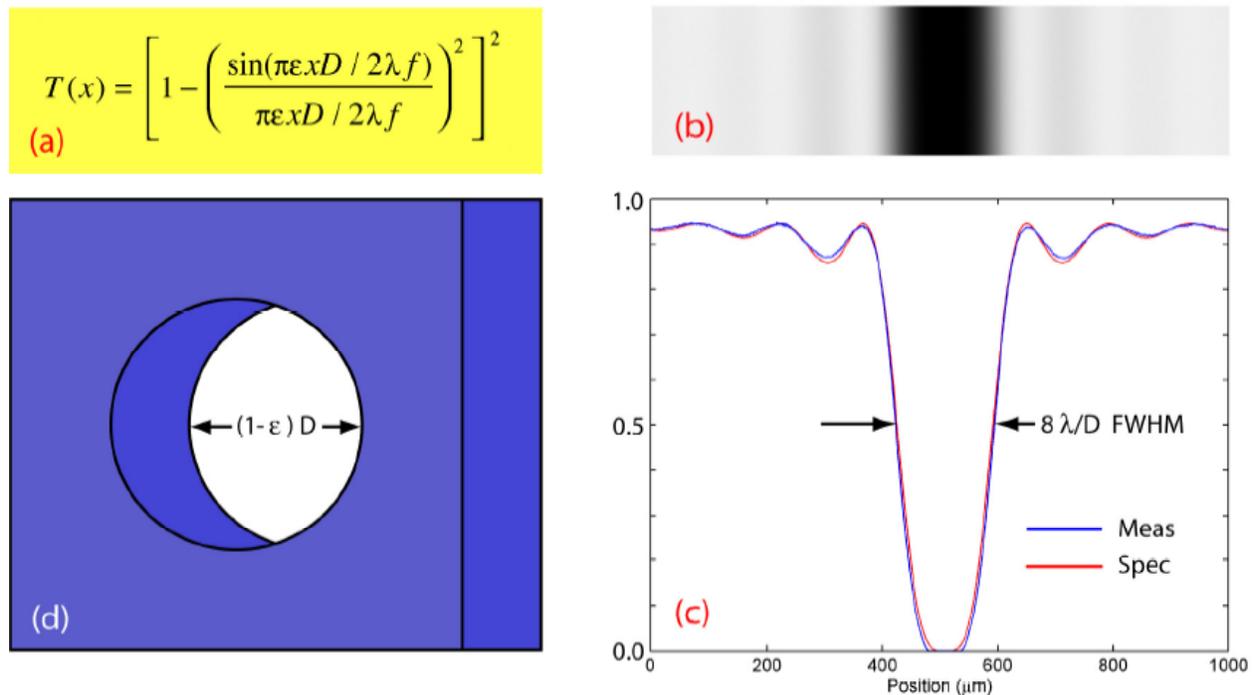
Figure 3. The coronagraph elements. *Collected here are: (a) the analytic specification for the attenuation profile of the linear coronagraph occulter; (b) a direct microscope image of the occulter as written by e-beam lithography in HEBS glass; (c) a plot of the achieved attenuation profile and comparison with the analytic specification; and (d) the geometry of the matching Lyot mask, fashioned from a pair of circular stops, each with opening diameter D and offset as indicated.*

4.0   MILESTONE PROCEDURES

Here we collect the various definitions, procedures, and requirements that comprise the TPF-C Milestone #1 demonstration, as specified in the Milestone White Paper (22 November 2005) and Amendment #1 (22 May 2006).

4.1   Definition of Terms

The M1 contrast metric requires a measurement of the intensity of speckles within the dark field relative to the intensity of the central star. Here we define the terms involved in the demonstration of M1.

Standard techniques for the acquisition of CCD images are used. We define a "raw" image to be the pixel-by-pixel image obtained by reading the charge from each pixel of the CCD, amplifying it, and sending it to an analog-to-digital converter. We define a "calibrated" image to be a raw image that has had background bias subtracted and the detector responsivity normalized by dividing by a flat-field image. Saturated images are avoided in order to avoid the confusion of CCD blooming and other potential CCD nonlinearities. All raw images are permanently archived and available for later analysis.

The "star" is a 5 μm diameter pinhole illuminated with narrowband light relayed via optical fiber from a source outside the HCIT vacuum wall (e.g. 785 nm radiation from a diode laser). This "star" is the only source of light in the optical path of the HCIT. It is a stand-in for the star image that would have been formed by a telescope system in TPF-C.

The speckle nulling "algorithm" is implemented in computer code that takes as input the measured speckle field image, and produces as output the voltage values to be applied to each element of the DM, with the goal of reducing the intensity of speckles.

The "contrast" metric is defined as follows. Let the image of a star be centered on a detector pixel. Let $T(i,j)$ be the transmission of the occulting mask that maps to the corresponding point on the detector, averaged over the area of the detector pixel, where (i,j) are the pixel coordinates. $T(i,j)$ is normalized to 1.0 at the first peak(s) in the transmittance profile. If S is the peak signal that would be measured in that pixel for a perfectly transmitting mask, then $S \times T(i,j)$ is the signal that would be measured (anywhere in the field of view) with a real mask. Likewise if P is the peak signal from a planet with a perfectly transmitting mask, then $P \times T(i,j)$ is the signal measured with a real mask. Both star and planet images pass through the same optical system, hence their PSFs are identical in all respects except peak brightness. The background field is dominated by speckles from the star. Let $B(i,j)$ be the measured background of speckles within a designated dark field area. Let $C_0 = P_0/S_0 = 10^{-9}$ be the target contrast between a star S_0 and a planet P_0 which is fainter by the factor C_0. Here S_0 and P_0 are the intrinsic brightness values, independent of our particular instrument. Let $V = <B(i,j)/T(i,j)>$ be the value of the average scaled background, where brackets indicate an average over all pixels in the target dark field area, and the $1/T$ factor scales up the measured brightness at a given point. The value of V is the speckle background contrast, the metric to be compared with the C_0 milestone criterion.

4.2 Contrast Photometry in Terms of the "Reference Planet"

(1) The occulting mask is laterally offset, so as to place the first maximum of its transmittance profile at the location of the star image.

(2) To create the photometric reference, a representative sample of short-exposure (e.g. 30 microseconds) images of the pinhole source is taken, with the coronagraph Lyot stop in place.

(3) The images are averaged to produce a single "reference planet" image. The peak value of this point spread function (PSF) is estimated, using either the value of the maximum-brightness pixel or an interpolated value representative of the apparent peak.

(4) A calibration is performed, with reference to the photometric images of the "reference planet", to determine the integrated detector counts received from the "planet" during the long (seconds) exposures required for the high contrast coronagraph images.

(5) The peak value is scaled, at this point or later, by the ratio of the "coronagraph contrast field" (defined below) detector counts to counts from the "reference planet". The term "peak value" should always refer to a value that is scaled appropriately and consistently for the context at hand.

(6) The "occulter transmittance profile" is measured using imaging data from a microscope CCD camera. This step is used to quantify the agreement between the occulter specification and its measured transmittance.

4.3 Each "Coronagraph Contrast Field" is Obtained as Follows:

(1) The occulting mask is centered on the star image.

(2) A long-exposure (e.g. seconds) image is taken of the coronagraph field (i.e. the suppressed star plus surrounding speckle field) with the Lyot stop in place. The dimensions of the dark field target areas are defined as follows: (a) A dark field extending from 4 to 10 λ/D, demonstrating a useful search space, is bounded by a line that passes 4 λ/D from the star at its closest point, and by a circle of radius 10 λ/D centered on the star. (b) An area within the foregoing dark field, demonstrating contrast at the inner working angle of 4 λ/D, is bounded by a square box, each side measuring 1 λ/D, such that one side is coincident with the foregoing line and centered on the closest point to the star.

(3) The image is divided by the occulter transmittance profile normalized to the first maximum in its transmittance profile.

(4) The resulting image is divided by the peak value of the reference star to produce a "contrast field" image.

(5) The contrast field image is averaged over each target high-contrast "dark field" area, to produce a "contrast metric" for each predetermined target area. The "average" is the sum of all of the pixel-by-pixel "contrast field" image values in the target area, divided by the total number of pixels in the dark field area, without any weighting being applied.

4.4   The Speckle Nulling Algorithm

We define "speckle nulling" to be the following eight-step process, iteratively repeated for as many cycles as are needed to reach a desired level of speckle suppression:

(1)   Measure the speckle field intensity in each pixel of the dark field or other target area in the focal plane;

(2)   Identify the speckles by location and brightness, and rank them by relative brightness;

(3)   Select a subset of these speckles for nulling: typically as many as 30 of the brightest speckles in the target area;

(4)   Compute a DM setting that will modulate the intensity of each of the selected speckles, exploiting the relationship between the spacing, orientation, and depth of the ripples in a sinusoidal grating and the "speckle" corresponding to the first order diffraction pattern of the star as dispersed by that grating. The DM setting is the superposition (sum) of up to 30 sinusoidal waves on the DM surface, each of which has a distinct wavelength, orientation, and amplitude on the DM surface as predetermined by the location and brightness of the corresponding speckle.

(5)   Compute three or more additional DM settings identical to that in step (4) but with modifications in the phases of the individual sinusoidal waves.

(6)   Apply this sequence of DM settings and measure for each the resulting speckle field;

(7)   Calculate and apply a new DM setting based on the resulting set speckle images;

(8)   Measure the speckle field intensity, expecting that it will be improved over the field measured at the start of this cycle.

4.5   The M1 Validation Procedure

(1)   DM voltages are initially set to a convenient bias level (e.g. 15 volts). The DM electroceramic actuators exhibit a displacement that is quadratic with voltage, hence a uniform bias voltage is applied to the DM to allow positive and negative actuator displacements. Speckle nulling is then performed to find settings of the DM actuator driver voltages that give an acceptable high-contrast wavefront solution for the target dark field. This typically takes from one to several hours, starting from scratch.

(2)   An initial contrast field image is obtained, as described in Section 4.4.

(3)   Subsequent contrast field images are taken, following the steps in Section 4.4, at the rate of about one speckle nulling cycle per 7.5 minutes, or about eight contrast field images per hour. The result at this point is a first set of eight contrast field images from a one-hour session.

(4)   Speckle nulling is then stopped, and the DM actuators are reset to a fixed uniform voltage for a period of 30 minutes. The setting of all actuators to a uniform voltage is the typical starting point for speckle nulling, hence the state of the DM has been returned to "scratch", defined here as a resting period of at least 30 minutes, during which time the voltages on the DM are set to a common value (15 volts bias applied to all DM actuators), and after which the DM actuators are returned to nominal voltages defined during previous DM calibrations.

(5)   Following the reset, the previously determined calibration voltages are again placed on the DM, and the system is allowed to settle for at least 30 minutes.

(6)   The speckle nulling cadence is restarted and continues until the coronagraph again achieves the required contrast, and then continues further for at least one hour, following steps 1–5 above. This produces a second set of about eight contrast field images from a one-hour session.

(7)   Step 6 is repeated, to produce a third set of eight contrast field images from a one-hour session.

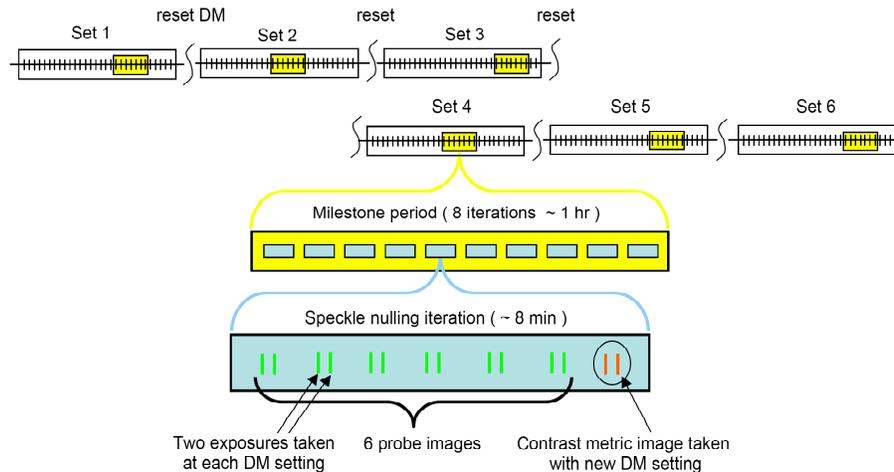(8)   The contrast metric is estimated for each contrast field image as described in Section 4.3.

Figure 4. The sequence of milestone demonstration images.

There is therefore a hierarchy of images, as illustrated in Figure 4, to which the following definitions apply. At any given DM setting, a pair of images is taken, each image of which is identical except for measurement noise and any small amount of instrument drift. Contrast for each DM setting is the average contrast from this "image pair". In each hour of speckle nulling activity, eight nulling iterations are completed and each iteration is scored with an image pair. These eight image pairs in each hour are referred to as a "set" of images. For the Milestone demonstration, six such "sets" are obtained. The ensemble of all six sets of eight image pairs is referred to as the "super-set" of images.

4.6   Statistics on the Contrast Metric

At any time in the demonstration, the HCIT contrast is subject to laboratory conditions, including the quality of the optical components, their alignment, any drift in their alignment over time, and the effectiveness of the speckle nulling wavefront sensing and control cycles. With each iteration, our speckle nulling procedure attempts to improve the contrast metric, and variations may be expected due to experimental noise and any limitations in the algorithm. The distribution of contrast metrics at each iteration is regarded as random about a mean contrast for the data set. We therefore consider the mean contrast as representative of the achieved contrast for a data set, and the distribution of contrast determinations among the eight DM settings for each set as a combination of both (random) speckle nulling variations and random measurement errors.

At each DM setting, a pair of images is taken. The contrast metrics (c_{i1} and c_{i2}) taken from each pair of images, which are expected to differ only due to statistical noise in the measurement, provide an estimate of the errors in the determination of contrast at the completion of each nulling iteration due to measurement noise (CCD read noise, shot noise, etc.) alone. The standard deviation for measurement noise σ_{meas} in the individual images is:

$$\sigma_{meas} = \sqrt{\sum_{i=1}^{n} \frac{(c_{i1} - c_{i2})^2}{2n}}$$

The contrast metric c_i at each DM setting is the average of the contrast metrics from the pair of individual images:

$$c_i = (c_{i1} + c_{i2})/2$$

The standard deviation in the average contrast c_i obtained by averaging the images in each image pair is therefore $\sigma_{meas}/\sqrt{2}$. The mean contrast for a set of eight images taken in a given hour is:

$$\hat{c} = \sum_{i=1}^{n} \frac{c_i}{n}$$

where $n = 8$ is the number of individual DM settings and image pairs in each set of images. The standard deviation σ_{each} in the contrast c_i obtained for each DM setting, which now includes both the measurement noise σ_{meas} and the (assumed random) contrast variations due to changes in the DM settings for each speckle nulling iteration, is:

$$\sigma_{each} = \sqrt{\sum_{i=1}^{n} \frac{(c_i - \hat{c})^2}{n-1}}$$

Our estimate of $\hat{c}$ is subject to the uncertainty in the contrast measurements $\sigma_{mean} = \sigma_{each}/\sqrt{n}$ and the overall errors in photometry σ_{phot}. The statistical confidence that the mean contrast $\hat{c}$ is less than $C_0 = 1 \times 10^{-9}$ is given by:

$$conf = \frac{1}{\sqrt{2\pi}} \int_{-\infty}^{t} e^{-z^2/2} dz$$

where $t = (C_0 - \hat{c})/\sigma$ and $\sigma = \sqrt{\sigma_{mean}^2 + \sigma_{phot}^2}$. As indicated in the first paragraph of this section, $\hat{c}$ and σ are the milestone metrics.

4.7   Success Criteria

Following is a statement of the eight elements required for a successful demonstration of the TPF-C M1. *Each element includes a brief rationale.*

(1)   Success is defined in terms of statistical confidence levels, a necessary consideration given the presence of noise and other uncertainties in the measurements. The objective is high confidence that the true value of contrast, as estimated from our measurements, meets the 10^{-9} requirement in each data set. The Milestone requirement, as amended (Appendicies 3 and

4), states that the estimated true contrast shall be obtained from the average of measured contrast values taken in each one-hour period (each data set) as defined below. By "high confidence" is meant that the true value of contrast meets the 10^{-9} requirement with a confidence coefficient of about 0.9 or greater. *As stated in Section 4.6, the mean contrast for each set constitutes our best estimate of the achieved contrast.*

(2)   A contrast metric of 1×10^{-9} or better must be achieved in a target dark field area ranging from 4 to 10 λ/D. *This requirement provides evidence that the high contrast field provides a useful search space for planets.*

(3)   A contrast metric of 1×10^{-9} or better must be achieved in a target dark field area ranging from 4 to 5 λ/D. *This tests whether there is a fundamental limitation at the inner working angle.*

(4)   Both (2) and (3) are to be satisfied simultaneously in each image. *Note that this requirement is modified by element (1), in that (2) and (3) are to be satisfied simultaneously in the mean of the images in each set.*

(5)   Illumination is spectrally narrowband (e.g. 0.785 μm laser light).

(6)   The contrast metric in (2) and (3) must be met in each successive contrast field image during a period of at least one hour. This is accomplished as follows: The speckle nulling algorithm will be used to repeatedly adjust the field of faint background speckles in the high-contrast target areas. Each successive high contrast image is the result of a speckle nulling sensing and control cycle that probes the speckle field by placing a sequence of (typically 6) small deformations on the deformable mirror. A new contrast field image is obtained approximately every eight minutes, at the end of each sensing cycle, for a total of about 8 images per hour. *This tests the robustness of the algorithm, i.e., that it does not get caught in local minima or depend on razor-edge alignments. Note that this requirement is modified by element (1), in that (2) and (3) are to be satisfied simultaneously in the mean over a period of at least one hour.*

A clarification regarding temporal stability: the background speckles are stable over the period of a speckle nulling sensing and control cycle (i.e. eight minutes). *While the position and intensity of the faint speckles in the background of the dark field are generally stable over extended periods (typically the average contrast drifts less than 10^{-11} per hour), maintaining contrast without running the algorithm is not planned. This would be a test of the stability of the laboratory environment rather than a test of the robustness of the algorithm, hence is not the intended purpose of this milestone.*

(7)   The above tests will be repeated 3 times, starting from "scratch".

This is a further test of robustness of the algorithm. This will be repeated to demonstrate achievement of the required level of contrast.

(8)   Demonstration of item (7) shall be repeated on a different day at least a few days later.

Finally, these success criteria are quantified in terms of the statistical contrast metrics $\hat{c}$ and σ defined in Section 4.6

5.0   NARRATIVE REPORT

Here we describe how each element of the milestone was met, with an explanation of the data obtained, analysis of the images and the contrast metric, illustrated with appropriate tables and

summary charts, and a narrative summary of the overall milestone achievement. We provide graphs and tables of the contrast metric for the inner and outer target areas in each contrast field image.

5.1   Definition of the Target Fields

There are two target fields. The exact location of these fields in the images is specified in pixel coordinates. The fields are sampled by the science CCD camera, a 1024 × 1024 pixel array with pixel dimensions of 13.0 × 13.0 microns. An f/77.4 beam illuminates the CCD, produced by a 30 mm diameter pupil stop at the DM and an effective focal length of 2322 mm. The f/no is therefore known in terms of the pupil diameter and focal lengths of the mirrors, and has been verified in science images in terms of the spacing of Airy rings in the PSF of the "star" with both the occulter and Lyot masks removed from the optical beam. Given the wavelength of 785 nm, the pixel scale at the CCD corresponds $\lambda/D = 4.67$ pixels. Hence $4\lambda/D = 18.7$ pixels, which we will round to 19 for the present purposes, in order to avoid the complications and errors associated with the sub-sampling of pixels. The inner 4–5 λ/D target field is a 5 × 5 pixel box including pixels 19–23 to the right of the centroid of the occulted star, extending vertically ± 2 pixels from the star centroid. The outer 4–10 λ/D target field includes all pixels 19 or more pixels to the right of the star and 47 or fewer pixels radially distant from the star. The inner box contains 25 pixels, the outer field contains 1771 pixels. The contrast metric is the average of the pixel-by-pixel contrast values over these two target fields.

5.2   Data Acquisition

The requirements described in elements (7) and (8) of Section 4.7 set forth a timeline over which the contrast is measured. Tables (1a) and (1b) indicate the times when data were taken to form each set, and when the DM resets took place. Sets 191-197 each span one hour, and were separated by 30-minute DM resets, as did sets 198–200. Set 191, which initiates the first sequence of three sets, began 3 days before set 198, which initiates the second sequence of three sets.

Table 1a. Acquisition dates and times for the first sequence of three data sets.
The starting and ending times for each one-hour set are shown. Between sets, the DM actuators were reset to a uniform 15 volts for 30 minutes.

Set	Date	DM voltage reset	Start	End
191	3/12/06	—	23:15	24:15
196	3/15/06	23:24–23:54 (3/14/06)	00:50	01:50
197	3/15/06	10:26–10:56	12:40	13:40

Table 1b. Acquisition dates and times for the second sequence of three data sets.
The starting and ending times for each one-hour set are shown.

Set	Date	DM voltage reset	Start	End
198	3/15/06	20:26–20:56	23:20	24:20
199	3/16/06	08:06–08:36	18:30	19:30
200	3/17/06	02:20–02:50	09:20	10:20

5.3   Photometry Ladder and Reference "Planet"

As outlined in Sections 4.2 and 4.3 above, the contrast image is derived from the coronagraph image, which is then corrected for the occulter attenuation profile and normalized with the PSF of the "reference planet". Figure 5a illustrates an average of three 30μs images of the planet PSF taken in sequence on 3/13/06, just following the completion of data Set 191, from which a peak intensity of 36200 (± 0.3%) DN is measured. Here the occulting mask has been laterally offset 144 microns to the first maximum in the transmittance profile (Figure 3c), and the Lyot mask (which is still in place) leads to a horizontal elongation in the PSF. Figure 5b illustrates a typical coronagraph image (it is the first image in Set 197) obtained with a 5-second exposure. Note that the presence of a rectangular field stop is now evident as the dark border around the speckle field of interest. It is located at an intermediate focal plane following the Lyot stop (Figure 1). The field stop is present at all times. A direct photometric comparison between the "planet" and the coronagraph fields for identical exposure times is not possible, since a 5 second exposure of the planet PSF would be far beyond the dynamic range of the CCD. Instead, a photometry ladder is used to estimate the peak intensity that the planet PSF would have had in a 5 second exposure, as detailed below. Then, a ratio is determined at one point in time between the planet intensity and a summation of all speckles within a fixed reference field (Figure 5c) in the coronagraph image outside the region controlled by the DM. The reference speckle field is insensitive to DM settings, and provides an internal reference to tie the planet PSF normalization to each coronagraph image.
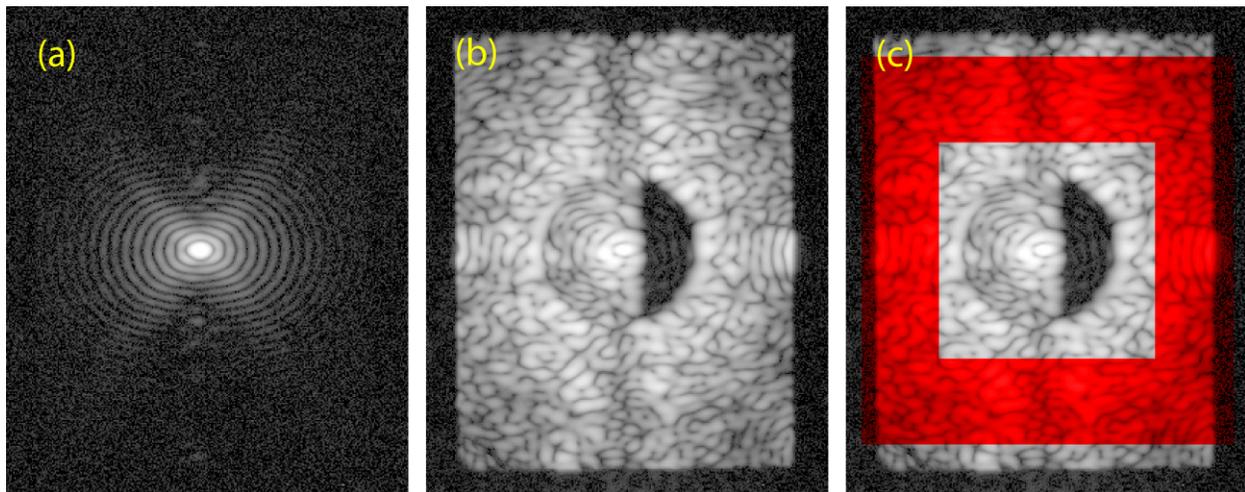

Figure 5.   Reference fields for contrast photometry. *Shown here are (a) the "planet" reference image; (b) the high-contrast coronagraph field bounded by a field stop at an intermediate focal plane; and (c) superimposed in red is the reference speckle field in the "uncontrolled" area beyond the Nyquist limit for the deformable mirror. All images are displayed with a logarithmic contrast stretch.*

The laser diode output is repeatable, but not strictly proportional to exposure time over the required 5-order-of-magnitude range in exposure times. The purpose of the photometry ladder is to determine the ratio between the peak signal in the "planet" PSF measured in a 30 μsec with the occulter removed and the peak value the PSF would have attained in an exposure as long as 1–5 seconds if the CCD had infinite dynamic range. Since the CCD response (electrons/detected

photon) is linear within 0.1% over a dynamic range of at least 50, the ratio can be obtained stepwise, as illustrated in Figure 6.
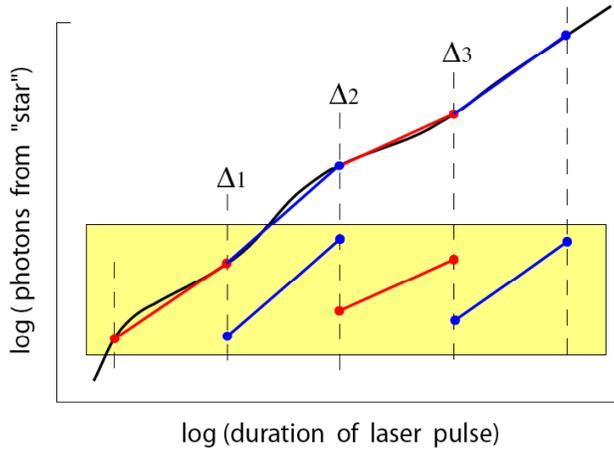

Figure 6. The photometry ladder. *This log-log plot shows schematically the relation between the number of photons generated by the diode laser (black curve) and the duration of the diode laser pulse. The integrated light ranges five orders of magnitude between the 30µs "planet" exposure (occulter mask moved to first transmittance maximum, Lyot mask in place) and typical 1–5 second coronagraph exposures, well beyond the dynamic range of the CCD detector (indicated by the vertical extent of the yellow box). Vertical dashed lines indicate points at which the integrated light is measured with a fixed pulse duration both before and after a physical attenuation of the "planet" flux. The photometry steps are indicated by the colored line segments, in which flux ratios are estimated over dynamic ranges consistent with the limits of CCD linearity.*

Table 2. Photometry Steps.

Flux ratios for the five-step photometry ladder
$I_1(300\mu s) / I_1(30\mu s) = 10.52 \pm 9.0\%$
$I_2 (3 ms) / I_2 (300\mu s) = 9.15 \pm 5.7\%$
$I_3 (30 ms) / I_3 (3 ms) = 16.3 \pm 4.5\%$
$I_4(1 sec) / I_4 (30 ms) = 28.2 \pm 3.0\%$
$I (5 sec) / I (1 sec) = 5.0 \pm 2.0 \%$
$I (5 sec) / I (30 \mu s) = 221200 \pm 12.1\%$
Steps of the photometry ladder
Five flux ratios were measured, as indicated in Figure 5, with the "planet light" physically attenuated keep the number of photons per pixel within the range of CCD linearity. Also listed are the standard deviations on the ratios derived from the scatter of photometry estimates among individual exposures that comprised each step in the ladder. The overall flux ratio between a 5-second laser pulse and a 30µs laser pulse is the product of the five ratios, as tabulated on the bottom line.

The photometry ladder was performed following the completion of data Set 200, with the results tabulated in Table 2. Attenuation was introduced at three steps in this procedure, as indicated by the vertical dashed lines with Δ symbols in Figure 5. Knowing that the laser output is independent of any attenuation introduced in the coronagraph optical path, arbitrary attenuation factors can be introduced to keep the CCD with its range of linearity for each pair of exposure times, and the incremental increase in integrated laser output can be measured at each step. The product of all five ratios is the ratio of PSF peak values between the 30μs reference exposure and the peak PSF value that would have been attained in five seconds if the CCD had an infinite linear dynamic range. Assembling these numbers, we estimate that the effective peak intensity for the "planet" PSF in a 5-second exposure would be $221200*36200 = 8.01 \times 10^9$ DN ($\pm$ 12%). Hence a signal level of 1 DN/pixel in the coronagraph high-contrast field, in a single 5-second exposure, corresponds to a contrast of $1.0/(8.01 \times 10^9) = 1.25 \times 10^{-10}$.

5.4   Image Analysis and Contrast Metrics

The contrast estimates require as input the coronagraph images, knowledge of the occulter profile, and the photometry reference derived from "planet" images. The images are reduced using standard CCD techniques. First, the bias level is estimated from a region of serial overscan in the CCD frame and subtracted from all pixels. The average dark count and spurious charge per pixel, estimated from dark images with equal exposure times, are subtracted from all pixels. No flat field corrections are made, since the CCD exhibits a pixel-to-pixel DQE uniformity of 1% or better. The analytic occulter profile, which is an excellent match to the measured attenuation profile (Figure 3), is multiplied by the estimated peak value of the "planet" PSF to generate a normalization image. The entire coronagraph image is then divided by this normalization image to produce a "contrast image".

Contrast metrics for the inner and outer dark fields are obtained by averaging the pixel values over the appropriate field of pixels.

Each image is subject to measurement noise arising from photon shot noise, CCD read noise, dark counts, and spurious charge. Measurement noise can be predicted as an RSS of these independent random variables, and can be verified in terms of the statistical scatter in image pairs taken with a given DM setting. CCD signals are measured in data numbers (DN), which is proportional to the count of electrons. This constant of proportionality for the HCIT CCD, as determined by standard analysis of multiple images of a uniformly illuminated field, is 2.6 $\pm$ 0.1 electrons/DN. Following the photometry procedure described above, we determine that a 1 DN/pixel signal in a 5 second exposure corresponds to a contrast value of 1.3×10^{-10}. Combining a measured read noise of 2.35 DN rms, dark+spurious charge of 0.75 DN, and shot noise corresponding to a typical contrast of 8×10^{-10} (approximately 6.40 DN / 5 second exposure) respectively, and converting to electrons/pixel, the measurement noise is predicted to be:

$$\sigma = \sqrt{6.11^2 + 1.95 + 16.64} = 7.5 \; electrons/pixel = 2.9 \; DN/pixel,$$

corresponding to a measurement uncertainty of 3.6×10^{-10} rms in each pixel, and a standard deviation of 0.7×10^{-10} for the contrast metric averaged over the 5×5 pixel area of the inner target.

This estimate has been tested by comparing image pairs, as indicated in Section 4.7. The directly measured estimate for σ_{meas} is 1.09×10^{-10} taken from the six data sets presented in this report, which is in reasonable agreement with the above prediction based on known sources of random noise. This

estimate for σ_{meas} is the origin of the error bars attached to the plotted contrast data points for the eight images in each of the six data sets below.

Measurement noise, contrast variations due to ongoing speckle nulling (assumed random), and the overall uncertainty in the photometry reference level are all RSSed together to estimate the contrast metric statistics. A graphic summary of the overall error budget appears as Appendix 1.

5.5   The Data Sets

The data are processed as outlined in the forgoing sections. To illustrate the procedure, we explicitly compute the contrast value in the inner 4–5 λ/D target area for the first image pair in Set 191. The steps are: (1) extract DN values for the 5 × 5 pixel inner target area, and estimate the bias and dark+spurious charge, (2) subtract the bias and dark+spurious charge from each pixel, (3) average the DN values for the two images in the pair, (4) extract the corresponding transmittance values from the occulter profile, (5) divide the DN values pixel-by-pixel by the occulter transmittance profile, (6) multiply by the planet reference normalization factor, and (7) average them over the 5 × 5 pixels and plot the result as the first data point in Figure 7. Step by step, the results are:

(1a)   For the first image of the first image pair in data Set 191.

The raw DN values for the inner target area (defined by columns 19 to 23, and rows –2 to +2, relative to the central occulted "star") are:

1876	1876	1874	1872	1871	DN
1879	1873	1873	1874	1871	
1870	1875	1872	1873	1874	
1874	1875	1873	1874	1880	
1873	1877	1875	1874	1868	

The bias averaged from 6000 overscan pixels = 1869.31 DN
Dark+spurious from 6000 pixels adjacent to overscan pixels = 0.81 DN

(1b)   For the second image of the first image pair in data Set 191:

The raw DN values for the inner target area are:

1873	1874	1874	1878	1870	DN
1875	1873	1876	1875	1872	
1876	1874	1871	1873	1875	
1871	1873	1877	1874	1873	
1875	1872	1875	1876	1878	

Bias averaged from 6000 overscan pixels = 1869.44 DN
Dark+spurious averaged from 6000 pixels adjacent to the overscan pixels = 0.73 DN

(2 & 3) Subtract bias and dark+spurious charge from each image in the pair, and average them:

4.36	4.86	3.86	4.86	0.35	DN
6.86	2.86	4.36	4.36	1.36	
2.86	4.36	1.36	2.86	4.36	
2.36	3.86	4.86	3.86	6.36	
3.86	4.36	4.86	4.86	2.86	

(4)   The analytic values for the occulter profile at these pixels are (Section 3.2):

    0.5191   0.5816   0.6427   0.7011   0.7558
    0.5191   0.5816   0.6427   0.7011   0.7558
    0.5191   0.5816   0.6427   0.7011   0.7558
    0.5191   0.5816   0.6427   0.7011   0.7558
    0.5191   0.5816   0.6427   0.7011   0.7558

(5)   The pixel DN values divided by the occulter profile:

     8.39   8.35   6.00   6.92   0.47 DN
    13.21   4.91   6.78   6.21   1.79
     5.50   7.49   2.11   4.07   5.76
     4.54   6.63   7.55   5.50   8.41
     7.43   7.49   7.55   6.92   3.78

(6)   Normalize to the planet reference by multiplying by 1.25×10^{-10} / DN (Section 5.3)

    1.05e-09   1.04e-09   7.50e-10   8.66e-10   5.87e-11
    1.65e-09   6.14e-10   8.47e-10   7.76e-10   2.24e-10
    6.87e-10   9.36e-10   2.64e-10   5.09e-10   7.20e-10
    5.67e-10   8.29e-10   9.44e-10   6.87e-10   1.05e-09
    9.28e-10   9.36e-10   9.44e-10   8.66e-10   4.72e-10

(7)   Giving the 5×5 pixel average contrast = 7.69×10^{-10}, which is plotted as the first contrast point in the Run 191 data plot in Figure 7.

    The computation of all contrast values, for inner and outer target areas, is carried out in like manner. For reference, the inner and outer data values for this image pair is included in Appendix 2.
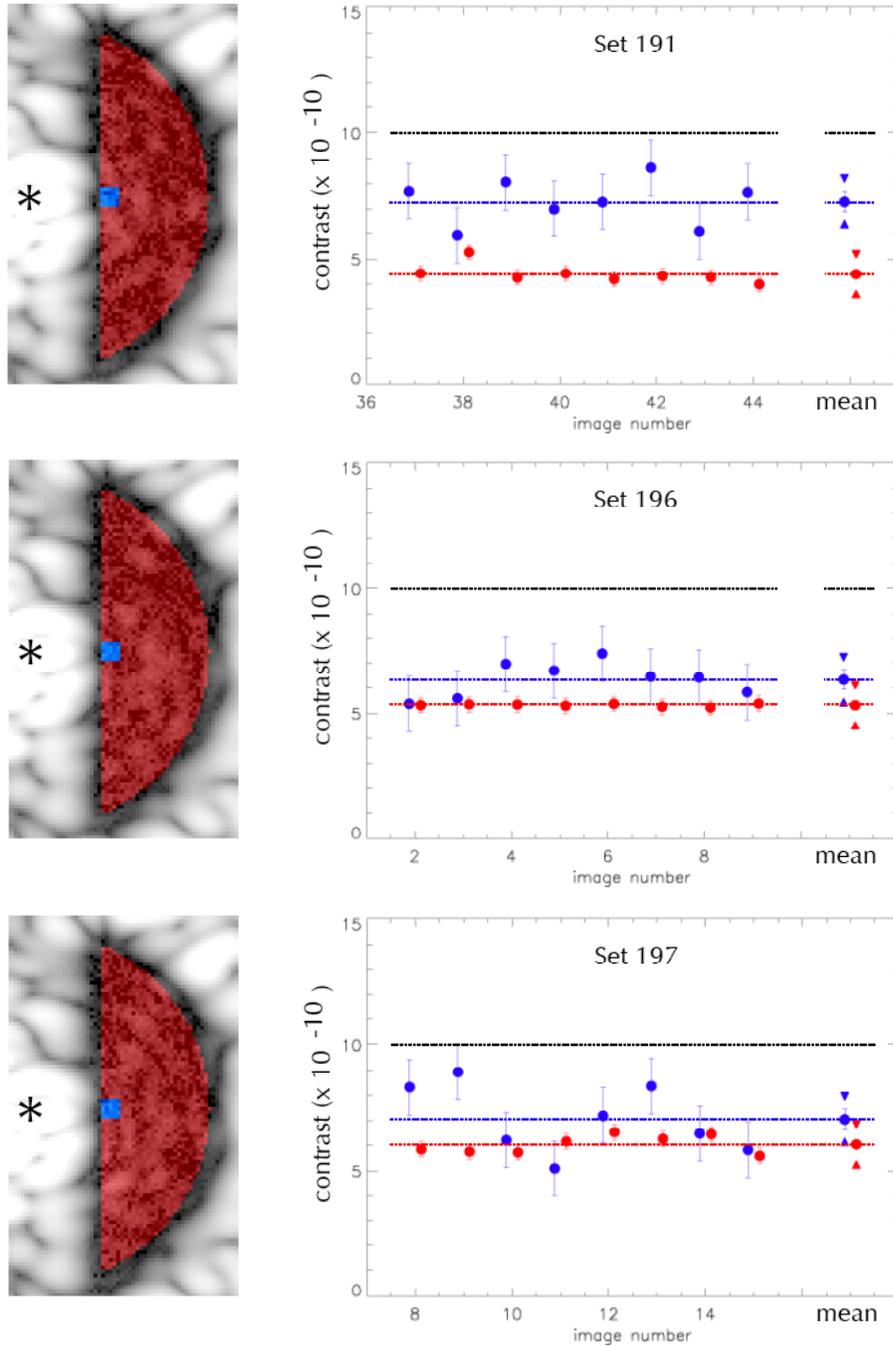
Figure 7a. The first sequence of three contrast data sets. *At left is the first image of each data set: the inner and outer target areas are highlighted in blue and red respectively; an asterisk marks the location of the occulted star. Plotted on the right (in blue and red, respectively) are the contrast values averaged over the inner and outer areas for each image in the set, with one-sigma error bars to indicate the measurement noise σ_{meas} (defined in Section 4.6). At far right in each plot is the mean contrast $\hat{c}$ for the data set. For the mean contrast, error bars indicate the standard deviation of the mean; triangle symbols indicate the larger one-sigma estimates when photometry errors are included. These estimates on the mean also appear in Table 3.*
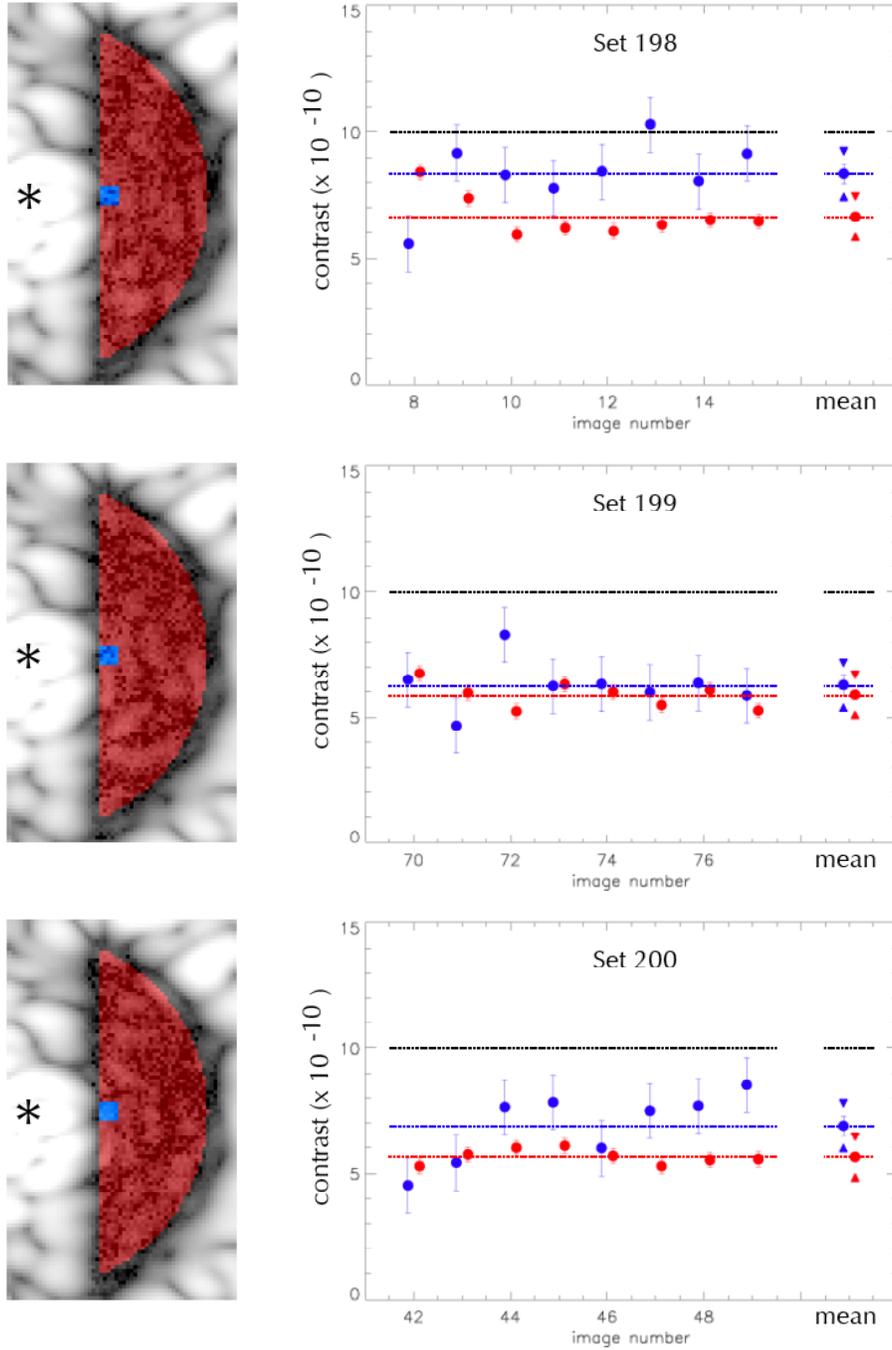
Figure 7b. The second sequence of three contrast data sets. *Images and plots are the same as for the previous figure.*
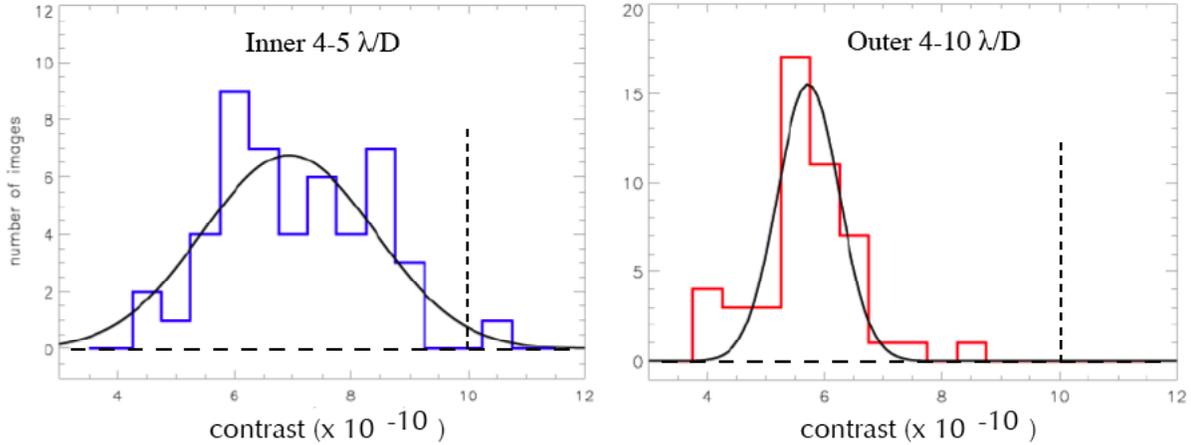
Figure 8. Histogram of contrast values. *The "super-set" of 48 individual contrast measurements, as plotted in Figure 7, are collected here as histograms for the inner and outer target areas. The vertical line indicates the 1×10^{-9} requirement on the mean contrast for each data set. Gaussians fit through the histograms confirm that the mean contrast is well within bounds for both the inner and outer areas.*

5.6   Summary of Contrast Metrics

The estimated contrast $\hat{c}$, the standard deviation σ, and confidence levels estimated for each of the six data sets, including measurement noise, ongoing speckle nulling variations, and photometry errors, are collected from the foregoing Section and tabulated in Table 3. We observe that the mean contrast in individual data sets can vary over a weeklong period in response to various physical conditions in the laboratory, including slow drifts in the laboratory temperature and optical alignment that can compete with the nulling algorithm's convergence rate. As illustrated in Figure 8, the superset of all data are nevertheless within Milestone requirements.

Table 3. Contrast Summary.

Set No.	Inner 4-5 λ/D			Outer 4-10 λ/D		
	$\hat{c}$ ($\times10^{-10}$)	σ ($\times10^{-10}$)	*conf*	$\hat{c}$ ($\times10^{-10}$)	σ ($\times10^{-10}$)	*conf*
191	7.3	0.9	99.9%	4.6	0.6	99.9%
196	6.3	0.8	99.9%	5.6	0.7	99.9%
197	7.1	1.0	99.8%	6.3	0.8	99.9%
198	8.3	1.1	93.9%	7.0	0.9	99.9%
199	6.3	0.8	99.9%	6.2	0.8	99.9%
200	6.9	1.0	99.9%	5.9	0.7	99.9%

Collected here for each of the six image sets are the mean contrast $\hat{c}$ ($\times 10^{-10}$), the standard deviation σ ($\times 10^{-10}$) on the mean for each set, all expressed in terms of the contrast metric, with the statistical confidence that the mean contrast is better than 1×10^{-9} in each set.

6.0   CONCLUSIONS

This report has described the HCIT layout, the nature of the HCIT data, procedures for the calibration of the images and estimation of the contrast metrics, and our results.

Table 3 contains our estimate $\hat{c}$ for the mean achieved contrast, the standard deviation σ in the scatter among individual DM settings due to both algorithm and measurement noise, and the statistical confidence *conf* that the mean achieved contrast is better than the 10^{-9} requirement.

We conclude that the TPF-C Milestone #1 has been demonstrated, since all confidence limits in Table 3, for both the inner and outer target dark fields, are nearly all above 0.99 and easily exceed the required "about 0.9 or greater". Furthermore, we note that the mean contrast for the super-set of all data, as indicated in the gaussian fits to the histograms of Figure 8, are 6.9×10^{-10} and 5.7×10^{-10} for the inner and outer target areas respectively, contrast values well within the milestone contrast requirement.

In summary, the HCIT coronagraph has achieved, repeatedly, contrast levels better than 10^{-9} at distances from a central "star" of relevance for future planet finding missions, and has demonstrated that the wavefront sensing and control algorithm can maintain this contrast in hour-long data sets as required by the milestone specification.

Appendix 1. HCIT CONTRAST MEASUREMENT ERROR BUDGET

Considering the major noise and error sources in the HCIT testbed we can estimate the expected variation in the contrast measurements. This estimate does not include the fact that the contrast measurements are taken with speckle nulling applied between CCD images. Figure 9 shows the error tree for HCIT.
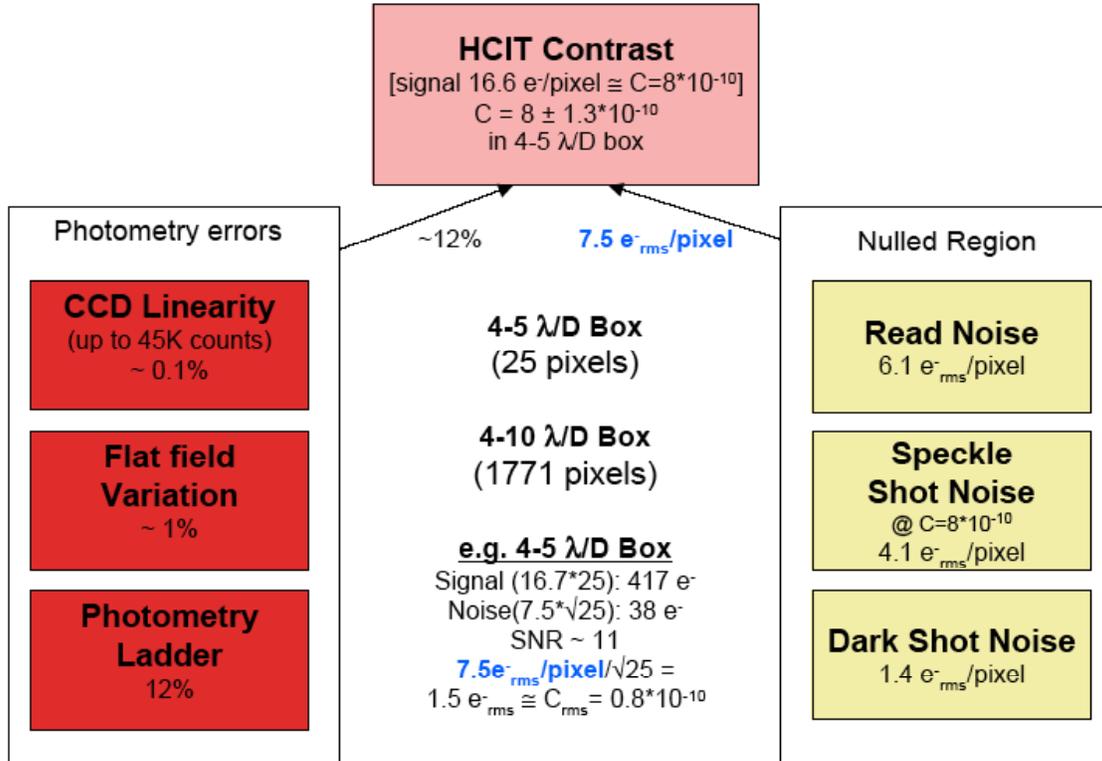

Figure 9. HCIT contrast measurement error tree. *HCIT error tree indicates the origin of the variations in the contrast measured in consecutive CCD images.*

The accuracy of the photometry ladder, the photometry error, includes the linearity of the CCD (estimated 0.1%), the knowledge of the CCD background (dark count and spurious charge) and the CCD variation in flat field response across the images (estimated 1%). The dark count is determined from a pixel-field that lies outside the field stop transmission. Since the dark count of 2.0 e$^-$/pixel is about 12% of the number of electrons for a contrast of $c = 8 \times 10^{-10}$, its error contributes about 1% to the total contrast error. The error in the measurement of the photometry ladder is estimated to be on the order of 12%.

The shot noise shown in Figure 9 is the shot noise at $c = 8 \times 10^{-10}$ and the read noise is as determined form the variance in the CCD bias region (serial overscan). The dark shot noise is the square root of the dark count. For a mean contrast of $c = 8 \times 10^{-10}$ the three noise sources and the photometry error of 12% result in a contrast variation for individual images of $\sigma_c \sim 1.3 \times 10^{-10}$.

Appendix 2. REPRESENTATIVE DATA

For clarification and reference, this appendix includes: (1) an image of the reference star, bias subtracted, (2) the specification of the occulter transmittance profile, and (3) a representative data array including both the inner and outer target fields in the coronagraph images, all with pixel coordinate scales traceable to units of Airy distance (λ/D).

Please insert Appendix foldout pages 2-1, 2-2, and 2-3 here.

Appendix 3. MILESTONE WHITE PAPER

TERRESTRIAL PLANET FINDER CORONAGRAPH

TECHNOLOGY MILESTONE #1 WHITE PAPER
NARROW BAND STARLIGHT SUPPRESSION DEMONSTRATION

November 22, 2005

Approvals

Prepared By:

John Trauger   11/30/05

John Trauger,
TPF-C HCIT Principal Investigator   Date

Approved By:

Dan Coulter   11/29/05

Dan Coulter,
TPF-C Project Manager   Date

Wesley Traub   29 Nov. 2005
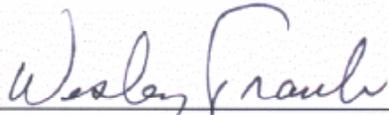
Wesley Traub,
TPF-C Project Scientist & Navigator Program Chief Scientist   Date

Michael Devirian   12/7/05
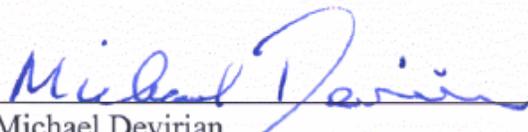
Michael Devirian,
Navigator Program Manager   Date

Z. Tsvetanov   1 Dec 2005
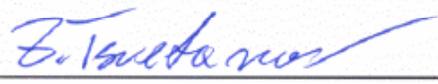
Zlatan Tsvetanov
TPF-C Program Scientist   Date

Lia S. LaP   Dec 6, 2005
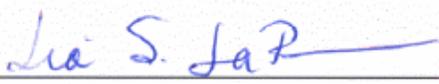
Lia LaPiana,
TPF Program Executive   Date

1

TPF-C Technology Milestone #1 White Paper: Narrow Band Starlight Suppression Demonstration

1. Objective

In support of the Terrestrial Planet Finder Coronagraph (TPF-C) pre-phase-A development program, this white paper explains the purpose of TPF-C Technology Milestone #1 (M1), specifies the methodology for computing the M1 metric, and establishes the success criteria against which the M1 metric will be evaluated.

2. Introduction

Technology Milestone M1 is one of three milestones established in the TPF-C Technology Plan (Version 1.1 dated 2 March 2005) to gauge the developmental progress of the High Contrast Imaging Testbed (HCIT) project and its readiness to proceed from pre-Phase A to Phase A. Completion of the milestones is to be documented by the project, reviewed by the TPF-TAC, and approved by NASA HQ. Milestone 1 addresses narrowband starlight suppression. It is discussed in the Technology Plan and reads as follows.

Milestone #1: Starlight Suppression

"Demonstrate that the High Contrast Imaging Testbed (HCIT) achieves a baseline contrast of $1x10^9$ (goal $1x10^{10}$) at a $4\,\lambda/D$ inner working angle, at $\lambda785$ nm and stable for at least one hour."

This metric addresses several key aspects of the TPF-C performance error budget. Following the recommendation of the TPF Science Working Group report in 2004, and as adopted in the engineering work on the Flight Baseline 1 (FB-1) observatory point-design, TPF-C is required to form a high contrast "dark hole" over a working angle spanning $4 - 40\ \lambda/D$ and a bandwidth of 500-800 nm. An extensive TPF-C modeling effort has shown that it is increasingly difficult to drive down the contrast of the dark hole as one moves toward the image of the target star. The HCIT testbed is addressing the most challenging location in the image plane, the inner working angle, at the same location required by TPF-C. The outer working angle for the flight mission is achieved using a large (at least 80 x 80 actuator) deformable mirror (DM). HCIT does not yet have a DM with this large format, so it is addressing a smaller region (out to 10 λ/D). This is of sufficiently large size that the physics of the wave front control problem can be demonstrated with high expectation of applying the same approach to a larger dark hole at a later date.

TPF-C must be capable of detecting light reflecting off of planets with intensity 10^{-10} fainter than that of the parent star. Ideally this is achieved by driving all scattered light surrounding the star to an intensity contrast ratio of scattered light to parent starlight that is below 10^{-10}. However, the expected contrast from the exo-zodiacal light may reach 10^{-9}. In pre-Phase A HCIT is required to demonstrate contrast reduction to the 10^{-9} level. By achieving this result, HCIT will have demonstrated performance that is limited not by the instrument but by the nature of the target. Technology Milestone M3 requires demonstration through modeling that the flight mission can achieve starlight suppression contrast of 10^{-10} adequate to detect terrestrial planets.

Speckles in the dark hole obey the same negative exponential statistics as laser speckle; the average intensity is equal to the standard deviation of the (spatial) intensity distribution. The distribution has a long tail – that is, there are bound to be a few very bright speckles. This is accounted for in the TPF-C performance error budget and is an expected result in HCIT. Because of this, the contrast specification relates to the average contrast level in the areas of interest around the source or parent star. Statistical measures of both the average intensity and its variation in a given dark hole area, and variations of both quantities among many dark hole realizations, will be provided in support of the Milestone 1 validation package, as specified in Sec. 4 below.

3. Computation of the Metric

3.1. Definitions

The M1 contrast metric requires a measurement of the intensity of speckles appearing within the dark hole, relative to the intensity of the incident star. In the following paragraphs we define the terms involved in this process, spell out the measurement steps, and specify the data products.

3.1.1. "Raw" Image and "Calibrated" Image. Standard techniques for the acquisition of CCD images are used. We define a "raw" image to be the pixel-by-pixel image obtained by reading the charge from each pixel of the CCD, amplifying it, and sending it to an analog-to-digital converter. We define a "calibrated" image to be a raw image that has had background bias subtracted and the detector responsivity normalized by dividing by a flat-field image. Saturated images are avoided in order to avoid the confusion of CCD blooming and other potential CCD nonlinearities. All raw images are permanently archived and available for later analysis.

3.1.2. "Scratch". We define "scratch" to be a resting period of at least 30 minutes, throughout which time the voltages on the DM are held at a common value (e.g., 20 volts on each actuator). The purpose of setting the DM to scratch is (a) to provide a neutral as well as standard starting point for subsequent DM operations, (b) to allow any transient

physical effects to relax to a negligible level, and (c) to provide a clean separation boundary between previous DM settings and those to follow.

3.1.3. "Star". We define the "star" to be a 5 μm diameter pinhole illuminated with narrowband light relayed via optical fiber from a source outside the HCIT vacuum wall (e.g. 785 nm radiation from a diode laser). This "star" is the only source of light in the optical path of the HCIT. It is a stand-in for the star image that would have been formed by a telescope system in TPF-C.

3.1.4 "Algorithm". We define the "algorithm" to be the computer code that takes as input the measured speckle field image, and produces as output a voltage value to be applied to each element of the DM, with the goal of reducing the intensity of speckles.

3.1.5. "Speckle nulling". We define "speckle nulling" to be the following eight-step process, iteratively repeated for as many cycles as are needed to reach a desired level of speckle suppression:
(a) Measure the speckle field intensity in each pixel of the dark hole or other target area in the focal plane;
(b) Identify the speckles by location and brightness, and rank them by relative brightness;
(c) Select a subset of these speckles for nulling: typically as many as 30 of the brightest speckles in the target area;
(d) Compute a DM setting that will modulate the intensity of each of the selected speckles: this will be the superposition of up to 30 sinusoidal waves on the DM surface, each of which has a distinct wavelength, orientation, and amplitude on the DM surface as predetermined by the location and brightness of the corresponding speckle.
(e) Compute three or more additional DM settings identical to that in step (d) but with modifications in the phases of the individual sinusoidal waves.
(f) Apply this sequence of four or more DM settings and measure for each the resulting speckle field;
(g) Calculate and apply a new DM setting based on the resulting set of four or more speckle images;
(h) Measure the speckle field intensity, expecting that it will be improved over the field measured at the start of this cycle.

3.2. Measurement of the Star Brightness

The brightness of the star is measured with the following steps.

3.2.1. The occulting mask is laterally offset, so as to place the first maximum of its transmittance profile at the location of the star image.

3.2.2. To create the photometric reference, a representative sample of short-exposure (e.g. 30 microseconds) images of the star is taken, with the coronagraph Lyot stop in place.

3.2.3. The images are averaged to produce a single star image. The "short-exposure peak value" of the star's intensity is estimated, using either the value of the maximum-brightness pixel or an interpolated value representative of the apparent peak.

3.2.4. The "peak count rate" (counts/sec) is measured for exposure time (sec) of micro-seconds to tens of second. This peak count rate, or an interpolated rate if the brightness changes with time, is then applied to any subsequent measurement of the speckle field, by multiplying by the exposure time of the latter measurement, and dividing the resulting value into the measured speckle intensities, to produce speckle intensities on a relative scale where the star image would have a peak value of unity. In this context, the term "peak value" always refers to a value that is scaled appropriately for the image at hand.

3.2.5. The "occulter transmittance profile" is measured using imaging data from a microscope CCD camera. This step is used to quantify the agreement between the occulter specification and its measured transmittance

3.3. Measurement of the Coronagraph Contrast Field

Each "coronagraph contrast field" is obtained as follows:

3.3.1. The occulting mask is centered on the star image.

3.3.2. A long-exposure (e.g. seconds) image is taken of the coronagraph field (i.e. the suppressed star plus surrounding speckle field) with the Lyot stop in place. The dimensions of the dark hole target areas are defined as follows: (a) A dark hole extending from 4 to 10 λ/D, demonstrating a useful search space, is bounded by a line that passes 4 λ/D from the star at its closest point, and by a circle of radius 10 λ/D centered on the star. (b) An area within the foregoing dark hole, demonstrating contrast at the inner working angle of 4 λ/D, is bounded by a square box, each side measuring 1 λ/D, such that one side is coincident with the foregoing line and centered on the closest point to the star.

3.3.3. The image is divided by the occulter transmittance profile normalized to the first maximum in its transmittance profile.

3.3.4. The resulting image is divided by the peak value of the reference star to produce a "contrast field" image, as discussed in Sec. 3.2.4.

3.3.5. The contrast field image is averaged over the predetermined target high-contrast "dark hole" area, or areas, to produce a "contrast metric" for each predetermined target area. To be explicit, the contrast metric is the sum of all of the pixel-by-pixel "contrast field" image values in the dark hole area, divided by the total number of pixels in the dark hole area, without any weighting being applied. The "rms contrast" in a given area can

3.4.10. Repeat steps 3.4.1. – 3.4.9. on a different day, at least 2 days later. The collection of about 60 images (30 per day) shall be known as the "super set" of data.

4. Success Criteria

The following is a statement of the seven elements that must be demonstrated to close TPF-C M1. Each element includes a brief rationale.

4.1. A contrast metric of 1×10^{-9} or smaller must be achieved in a target dark hole area ranging from 4 to 10 λ/D.

Rationale: *This provides evidence that the high contrast field provides a useful search space for planets.*

4.2. A contrast metric of 1×10^{-9} or smaller must be achieved in a target dark hole area ranging from 4 to 5 λ/D.

Rationale: *This tests whether there is a fundamental limitation at the inner working angle.*

4.3. Both (4.1) and (4.2) are to be satisfied simultaneously in each image.

4.4. Illumination is spectrally narrowband (e.g. 0.785 μm laser light).

4.5. Items 4.1 – 4.4 must be satisfied for each image in the super set of data.

Rationale: *This tests the robustness of the algorithm, i.e., that it does not get caught in local minima or depend on razor-edge alignments. This also tests the repeatability of the algorithm, i.e., that it will work at different times on different days, and is not simply a one-time fluke. Finally, this tests the robustness of the algorithm, i.e., that it can be cold-started from a scratch situation and still achieve an acceptable low level of contrast.*

4.6. A clarification regarding temporal stability: for the algorithm to work, the background speckles must remain stable over the period of a speckle nulling sensing and control cycle (i.e. 6 minutes).

Rationale: *While the position and intensity of the faint speckles in the background of the dark hole are generally stable over extended periods (typically the average contrast drifts less than 10^{-11} per hour), maintaining contrast without running the algorithm is not planned. This would be a test of the thermal and electronic stability of the testbed, and not the robustness of the algorithm, hence is not the intended purpose of this milestone.*

5. Certification Process

The TPF-C Project will assemble a milestone certification data package for review by the TPF-C TAC and the Navigator EIRB. In the event of a consensus determination that the success criteria have been met, the project will submit the findings of the review boards, together with the certification data package, to NASA HQ for official certification of milestone compliance. In the event of a disagreement between the project and the EIRB, NASA HQ will determine whether to accept the data package and certify compliance or request additional work.

5.1. Milestone 1 Certification Data Package

The milestone certification data package will contain the following explanations, charts, and data products.

5.1.1. A narrative report, including a discussion of how each element of the milestone was met, an explanation of each image or group of images, appropriate tables and summary charts, and a narrative summary of the overall milestone achievement.

5.1.2. Calibrated images of the reference star.

5.1.3. Calibrated images of the occulter transmittance profile.

5.1.4. Calibrated images of the super set of data, with appropriate numerical or color-coded or grey-scale coded contrast values indicated, and with coordinate scales indicated in units of Airy distance (λ/D), all in demonstration of achieving the milestone elements.

5.1.5. A contrast metric value for each target area in each contrast field image, i.e., the super set of data, in tabular form.

5.1.6. Statistical data on the super set, including the global average metric value and associated uncertainty, as well as a summary of the average scatter within each data set and among all images in super set.

Appendix 4. AMENDMENT TO MILESTONE WHITE PAPER

Subject: RE: HCIT milestone amendment #1
Date: Mon, 22 May 2006 10:54:16 -0400
From: "LaPiana, Lia S. \(HQ-DE000\)" <lia.s.lapiana@nasa.gov>
To: "Wesley A Traub" <Wesley.A.Traub@jpl.nasa.gov>
Cc: <Marie.B.Levine-West@jpl.nasa.gov>, <John.T.Trauger@jpl.nasa.gov>,
     <wtraub@jpl.nasa.gov>, "Lia LaPiana" <llapiana@hq.nasa.gov>,
     "Tsvetanov, Zlatan \(HQ-DE000\)" <zlatan.tsvetanov@nasa.gov>

Looks good! Thanks

Lia

+++
Lia S. LaPiana
NASA Headquarters
Science Mission Directorate
Astrophysics Division
Mail Suite 3W39
Washington, DC 20546-0001
Office: 202-358-0346
Fax: 202-358-3096
Email: Lia.S.LaPiana@nasa.gov
+++

-----Original Message-----
From: Wesley A Traub [mailto:Wesley.A.Traub@jpl.nasa.gov]
Sent: Friday, May 19, 2006 6:05 PM
To: LaPiana, Lia S. (HQ-DE000)
Cc: Marie.B.Levine-West@jpl.nasa.gov; John.T.Trauger@jpl.nasa.gov;
wtraub@jpl.nasa.gov
Subject: HCIT milestone amendment #1

Lia:

As you requested, we revised the proposed version of the HCIT Milestone
#1 amendment to include a specific reference to the need for a
statistical confidence coefficient. This was implicit in the previous
version, but is explicit now. Please let me know if this version is
acceptable.

Wes

Amendment #1. For the purposes of Milestone #1, as described in this
white paper, the interpretation of numerical values of measured contrast
values shall take into consideration, in an appropriate way, the
statistics of measurement, including for example detector read noise,
photon counting noise, and dark-count noise.

The goal is high confidence that the true value of the contrast in the
dark hole, as estimated from our measurements, is less than the required
threshold contrast value C_0. The estimated true contrast shall be
obtained from the average of the set of approximately eight measured
contrast values obtained in a one-hour period, corresponding to
approximately eight individual DM settings. For this milestone, the
required threshold is $C\_0 = 1.0 \times 10^{-9}$.
By "high confidence" we mean a confidence coefficient of about 0.90 or
better.

_____

Wesley A. Traub   wtraub@jpl.nasa.gov
Chief Scientist, Navigator Program
Project Scientist, Terrestrial Planet Finder Coronagraph
Cell: 818-726-2462   Work: 818-393-5508   Fax:
818-393-4950
Jet Propulsion Lab, M/S 301-451, 4800 Oak Grove Dr., Pasadena CA, 91109

_____